

**ELECTRON ACCUMULATION IN THE PSR:
AN ATTEMPT TO UNDERSTAND THE BASIC
FACTS.**

SNS/ORNL/AP TECHNICAL Memo

A. Aleksandrov, V. Danilov,
ORNL SNS Project, Oak Ridge, TN 37831
M. Blaskiewicz,
BNL, Upton, NY 11973

May 10, 2000

Spallation Neutron Source Project
Oak Ridge National laboratory
701 Scarborough Rd. MS 6473
Oak Ridge TN 37830

ELECTRON ACCUMULATION IN THE PSR: AN ATTEMPT TO UNDERSTAND THE BASIC FACTS

A. Aleksandrov, V. Danilov,
ORNL SNS Project, Oak Ridge, TN 37831

M. Blaskiewicz,
BNL, Upton, NY 11973

The Proton Storage Ring (PSR) in Los Alamos has a fast intensity-limiting instability, which may result from an electron cloud interaction with the circulating proton beam leading to a transverse mode coupling instability. The most probable mechanism of the electron creation is multipacting. Though the effect depends on many parameters, simple models of multipacting are presented for the coasting and the bunched proton beam. The comparison between simulations and experiments is given. It is shown that basic facts about electron detector signals for the bunched proton beam could be related to two possible mechanisms of electron creation.

INTRODUCTION

The LANL PSR has a fast instability that limits the proton beam intensity per pulse. A probable explanation of this instability is that there exists a large electron density in the vacuum chamber resulting in an electron interaction with the proton beam leading to a transverse mode coupling instability between the circulating protons and oscillating electrons trapped in the proton potential well. Multipacting can drastically increase the electron density, increasing the instability rates. This physical phenomenon has different signatures in two of the cases, either a coasting or a bunched proton beam.

(1) For the coasting beam, the multipacting occurs due to the proton beam instability. Electrons could accumulate during beam injection in the proton beam potential well, and after reaching some threshold density, could generate unstable coupled oscillations between themselves and the proton beam. In this case the lighter electrons gain large amplitudes and strike the vacuum chamber wall, producing an avalanche of secondary emission (SEM) electrons, resulting in the large transverse amplitudes of the protons [1].

(2) For the bunched beams there are two scenarios for the electron accumulation - single pass and multi-pass electron accumulation.

a) Single pass accumulation is related to the multipacting on the trailing edge of the proton beam. For the case of a constant longitudinal density, electrons with zero initial kinetic energy at the vacuum chamber wall oscillate across the vacuum chamber gap through the circulating beam with zero energy gain. If the longitudinal bunch density is increasing the electrons lose their energy. If the longitudinal bunch density is decreasing, the electrons gain energy after traversing the vacuum chamber. It is speculated that multipacting can

significantly increase the number of electrons on the trailing edge of the proton bunch if the energy gain of the electrons is above 50 eV for an aluminium vacuum chamber. If at some point there is a significant number of electrons at the vacuum chamber while the proton beam center passes, this number of electrons will be increased by a tremendous factor, depending on the material of the wall. Electrons, existing due to beam losses or other reasons, produce an avalanche of the secondary emission electrons. The process continues up to the point when the electron density is comparable with the density of the proton beam. It is probable that this mechanism works at the stripper foil point, where the density of electrons is high from the very beginning, and at the ceramic and aluminum parts of the vacuum chamber with high SEM coefficient. Almost all electrons accumulated at single pass disappear in the beam gap due to their own space charge.

b) Multi-pass accumulation of electrons has more complicated origin. If the SEM coefficient (or the number of initial electrons at the wall) is low enough to produce any significant electron density during a single pass, these electrons can accumulate due to multi-turn process. In the first significant papers on PSR instability (see, e.g. ²) there is an assumption that some mechanisms, for electrons to be stable in the strong field of the bunched proton beam, should exist. For example, some portion of the proton beam in the gap was listed as a probable candidate for this mechanism.

Our claim is that all those mechanisms are too subtle to explain the repeatability of the electron accumulation and the e-p instability. In the strong fields of the bunched proton beam electrons become unstable when the proton intensity is high enough. According to the kinematics of electron motion, all electrons existing in the gap are attracted to the center of the proton beam when it is passing through. On the trailing edge of the proton beam, electron amplitude increases and electrons hit the wall near the very beginning of the proton beam gap. When there is high enough proton intensity, electron energy is enough to produce more than one electron on average. The secondary particles travel across the vacuum chamber at low velocities and can survive the gap without hitting the wall again. Then the same events happen many times with slow accumulation of the electron density. If the electron density were high enough to repulse the secondary electrons in the gap back to the wall, the accumulation would stop. This corresponds to the saturation of electron density.

All the mentioned above scenarios for electron accumulation are presented in the following sections with their correspondent comparison with the experimental data from electron detectors. However, we must first present the experimental evidence that the secondary emission influences the electron accumulation.

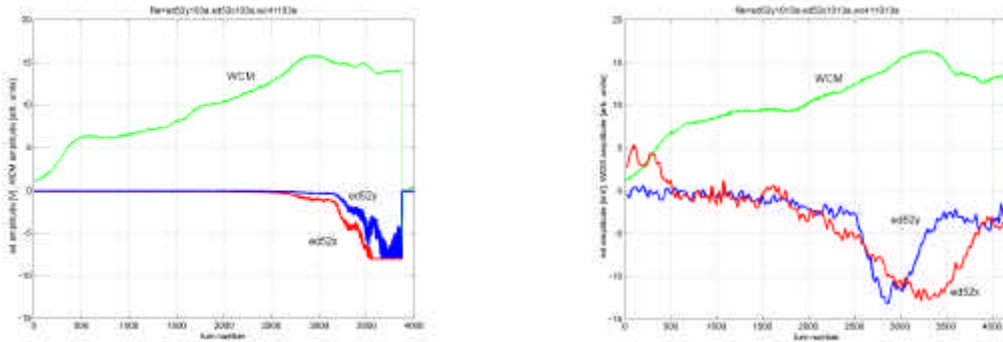
ELECTRON DETECTOR SIGNALS: STAINLESS STEEL VERSUS TiN COATED VACUUM CHAMBERS

In order to measure the electron density and the time dependence of the electron flux, the PSR vacuum chamber was equipped with electron energy analyzers with two mesh grids in front of an electron collector. Basically the experimental setup and the detectors are copied from those of the Argonne Photon Source (APS) storage ring³, with adjustments of sizes to

the 4" PSR vacuum chamber. The proposal to use electron detectors for PSR, as well as to coat the PSR vacuum chamber piece with the Ti N was made by R.Kustom⁴.

The detector signals were distinctly found at all locations. The strongest signals were observed near the stripper foil and current transformers with ceramic insertions. In order to check if the electron signal depends on the secondary emission from the wall surface, two similar 109" long pieces of the vacuum chamber were manufactured, both made of stainless steel. One piece was coated with the Titanium Nitrate (TiN) by Berkeley and SLAC physicists. This material has a low Secondary Emission (SEM) coefficient with its maximum of about 1 after a conditioning. The stainless steel SEM coefficient at its maximum is about 2, so the materials should have a significantly different multipacting effect.

To coat the vacuum chamber the following process was used^a. A titanium rode was inserted into the vacuum chamber piece. With a pressure in the vacuum chamber of about 100 μ Torr of gasses Nitrogen (30%) and Argon (70%), a high voltage was applied to the titanium rode for approximately one hour. Due to glow discharge the Titanium sputtered in the chamber and covered the stainless steel, giving a bronze color to the chamber surface (the estimated thickness of the Ti N layer is about 1 μ m). Nitrogen molecules bonded to the Titanium molecules forming a surface coating resistant to chemical processes (such as oxidation, etc.). To prevent absorption of the air molecules, the coated pipes were backfilled with nitrogen, shipped to Los Alamos, and installed at the PSR.



a)

b)

Figure 1 Signals from electron detectors (blue for vertical and red for horizontal ones) for the stainless steel (a) and TiN coated (b) vacuum chambers. The scale for the red and blue lines on the left figure is 1000 larger than for the right one.

Figure 1 represents the signals from the wall current monitor (green lines) and from vertical (blue lines) and horizontal (red lines) detectors. The wall current monitor signal is shown in the same units in figures a) and b) and its maximum corresponds to

^a The coating was done in SLAC with the same equipment that was used for the SLAC B-factory.

approximately 8 μC of accumulated proton charge. The scale of the electron detector signals is 1000 times smaller for figure b) - its signals are given in milliVolts (one Volt of this signal roughly corresponds to 0.1 mA of the detector current^b). One can see that the TiN vacuum chamber has a signal approximately 1000 times less than the stainless steel one. It proves that the secondary emission plays a crucial role in the electron cloud formation.

COASTING BEAM PHENOMENA

In a stable coasting beam the electric and magnetic fields are constant in time. The electric field is derivable from a potential $\Phi(x,y,s)$, where x and y are the horizontal and vertical coordinates, respectively. Barring rapid changes in the vacuum aperture the length scale for variations in the longitudinal coordinate s is the distance between quadrupoles (L), which is much larger than the pipe radius (b). Therefore, the potential obeys the two dimension Poisson equation

$$\frac{\partial^2 \Phi}{\partial x^2} + \frac{\partial^2 \Phi}{\partial y^2} = -\frac{\mathbf{r}(x, y, s)}{\mathbf{e}_0}, \quad (1)$$

where $\Phi=0$ on the vacuum chamber walls. Both transverse and longitudinal electric fields are present with $E_s/E_\perp \sim b/L$. For a round beam with uniform charge density the potential drop between the center and edge of the beam is given by

$$d\Phi_b = \frac{Z_0 I}{4\pi b}$$

and with beam radius a the potential drop between the edge of the beam and the (round) vacuum chamber wall is

$$d\Phi_w = \frac{Z_0 I}{2\pi b} \ln(b/a).$$

Taking typical PSR values of $I=5$ A, $\beta = 0.84$, $a = 1$ cm, and $b = 5$ cm; $\delta\Phi_b= 178$ V and $\delta\Phi_w= 575$ V. Since both of these voltages are small compared to $m_e c^2/e = 511$ kV, the electrons are non-relativistic and the beam induced magnetic fields will have a small effect on the motion. The fields created by the bending and focusing magnets are less negligible. With a 1 Tesla dipole field the $\mathbf{E} \times \mathbf{B}$ drift allows an electron to traverse a 3 meter dipole in about 100 μs . Therefore it is reasonable to assume that electrons trapped by the beam are distributed around the ring. Electrons are generated by collisional stripping of residual gas, ejection from the vacuum chamber wall by lost protons and

^b Vacuum chamber has three slots for let electrons into detector. Two slots are 1/8x1/2" and one slot is of 1/8x5/8" size. One can estimate the electron current density with the given numbers.

through proton and H traversals of the stripping foil. For residual gas stripping the total number of electrons N_e satisfies

$$\frac{dN_e}{dt} = v_p \sigma_p n_g N_p + v_e \sigma_e n_g N_e,$$

where v_b is the beam velocity, σ_p is the cross section for ionization by protons, and n_g is the number density of background gas. The second term on the right estimates the rate at which electrons trapped by the beam can strip the background gas. Let the electron energy be $E = E_{100} / 100 \text{ eV}$ and the cross sections be in units of Megabarns, $\sigma_p = \sigma_{pMb} \cdot 10^{-22} \text{ m}^2$, and $\sigma_e = \sigma_{eMb} \cdot 10^{-22} \text{ m}^2$. Take the gas pressure to be $P = P_8 \cdot 10^{-8} \text{ Torr}$ and the temperature to be $T = T_{300} / 300 \text{ Kelvin}$. Then $v_e \sigma_e n_g = 0.191 \sigma_{eMb} \sqrt{E_{100}} P_8 / T_{300} \text{ s}^{-1} = 1/\tau_e$ and $v_p \sigma_p n_g = 8.11 \sigma_{pMb} \beta P_8 / T_{300} \text{ s}^{-1} = 1/\tau_p$. For stable conditions the pressure of the residual gas is $P_8 \sim 1$ and the cross sections are

$\sigma_{eMb} \sim 100$ and $\sigma_{pMb} \sim 1$, hence $\tau_e \sim \tau_p \geq 100 \text{ ms}$. A fractional neutralization of a few percent is possible in one millisecond.

Protons lost at the vacuum chamber wall will eject electrons from the metallic surface. For an 800 MeV proton of order 100 electrons could be generated from a single lost proton⁵. These electrons will have large amplitudes and may strike the vacuum chamber after a few oscillations through the beam. For stable beam the total electron energy is conserved and it is likely that the electrons impact with $\leq 10 \text{ eV}$. The final source of electrons is the stripper foil. There are two, 400 keV electrons created when an H is stripped. These high energy electrons are not trapped by the beam electric field and strike the vacuum chamber wall after hitting any significant magnet field. Multiple passages of the proton beam will heat the foil, leading to thermionic emission. Protons also can knock out electrons through Coulomb scattering events. For the PSR thermionic emission leads to less than 2 % neutralization, while Coulomb scattering events in the foil can create 6 electrons per stored proton⁶. Coupled with the $\mathbf{E} \times \mathbf{B}$ drift this last effect could lead to 100 % neutralization of the proton beam in less than a millisecond. This last observation is consistent with the large electron fluxes measured near the PSR stripping foil and is of major concern for the SNS. After electrons have accumulated to a sufficient degree a two stream instability results. In linearized theory the electron amplitude Y_e is related to the proton amplitude Y_p by $Y_e / Y_p \sim f_e / f_{rev}$ where f_e is the electron bounce frequency and f_{rev} is the revolution frequency. Normally, $f_e \gg f_{rev}$ so electrons will strike the wall well before the proton beam gains sufficient amplitude to cause losses. If the electrons are lost at the walls the instability will stop and a slight increase in proton emittance will be observed, as in the ISR⁷. The instability seen in the AGS Booster and PSR is much more violent so there must be some mechanism to replace electrons, which hit the walls. Theories involving secondary electron emission have been developed⁸ and they are in reasonable agreement with the data.

ELECTRON ACCUMULATION FOR THE BUNCHED BEAM

Electron accumulation in a storage ring could happen for many reasons. If the bunching were weak, it would make the electron motion stable and the coasting beam phenomena applicable in this case. However, the PSR bunch length, the revolution frequency, and the proton beam intensity make the electron motion far from stable. Only very smooth (e.g. Gaussian) longitudinal distributions of the proton beam (or some significant amount beam in the gap) can guarantee the electron stability only if the electron motion is linear. If one take into account nonlinear fields of the proton beam, the stability area will shrink to negligible sizes (about 1 mm), making the motion for most of the phase space unstable and chaotic⁹. Starting without any assumptions on electron stability, we will present two different scenarios for the electron creation and accumulation. Both scenarios are related to the multipacting process. Thus, the electron motion should be unbounded at small apertures. Moreover, the larger increment of electron instability, the stronger the process.

SINGLE PASS ELECTRON ACCUMULATION

The first mechanism of the electron accumulation is related to the multipacting on the trailing edge of the proton beam. On the trailing edge of the proton bunch, longitudinal bunch density is decreasing and the electrons gain energy. If there are many electrons from the beam losses at the longitudinal center of the bunch, or if the secondary emission coefficient is large, the electron cloud density could reach the density of the proton beam. Almost all electrons accumulated at single pass disappear in the beam gap due to their own space charge. These effects are estimated in this section.

To investigate it, a computer code was created that calculates 1D electron trajectories, starting from the vacuum chamber wall. After striking the wall, secondary emission electrons are produced depending on the primary initial energy. The secondary electrons start to oscillate with zero momentum in the proton potential since their initial energies are small in comparison with the average single-pass energy gain in the proton potential, about 100 eV.

Figure 2 shows one example of electron motion (solid line) with respect to the proton bunch distribution (dashed line). The zero longitudinal coordinate corresponds to the center of the beam gap, the initial electron vertical coordinate is about the vacuum chamber radius of 5 cm, and the initial distance between the gap and the electron is 38 meters. One can see that initially the electron oscillation amplitude decreases due to the proton beam density increase. Once the proton beam center has passed the electron, the transverse amplitude increases and the electron finally hits the wall several times, losing all its energy with each wall hit. The total number of secondary emission electrons is summed over all the collisions

with the vacuum chamber using the formula for secondary emission yield $y(E)^{10}$, assuming the primary electrons are normal to the surface. That is:

$$y(E) = y_{\max} 1.11(E/E_m)^{-0.35} (1 - e^{-2.3(E/E_m)^{1.35}}) \quad (2)$$

where $E_m = 400\text{ eV}$, y_{\max} depends on the vacuum chamber material. The proton beam transverse distribution is taken to be constant within the beam radius, and equal to zero otherwise.

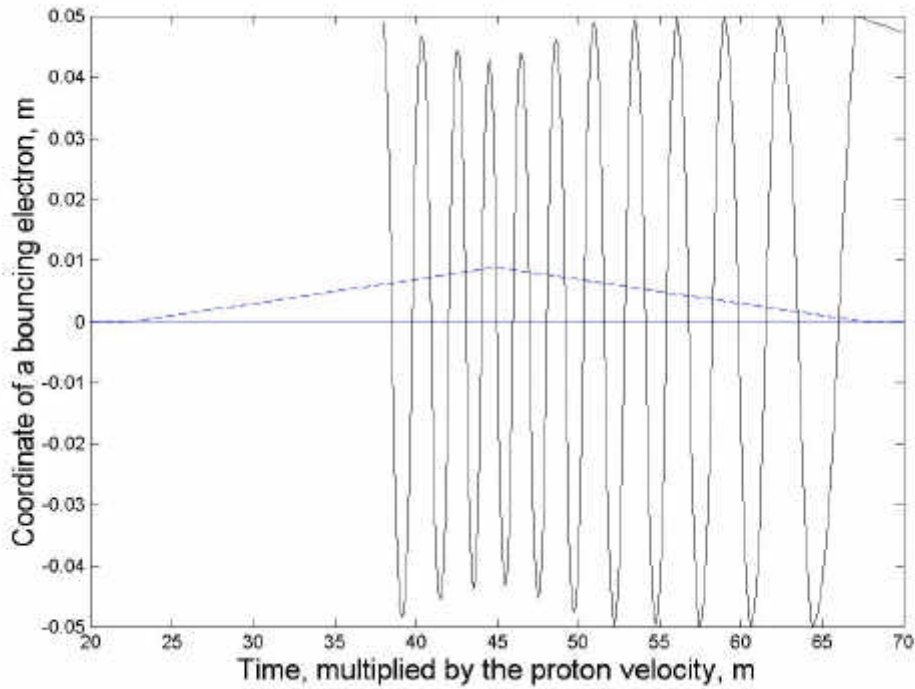


Figure 2 Coordinate of an electron oscillation in the electric field of proton beam.

The final result is presented as the secondary emission (SEM) factor, which is the natural logarithm of the average number of electrons produced by one initial electron. The initial time of the test electron oscillation corresponds to the center of the proton bunch passing. The final time corresponds to the moment when this number of produced secondary emission electrons is maximal.

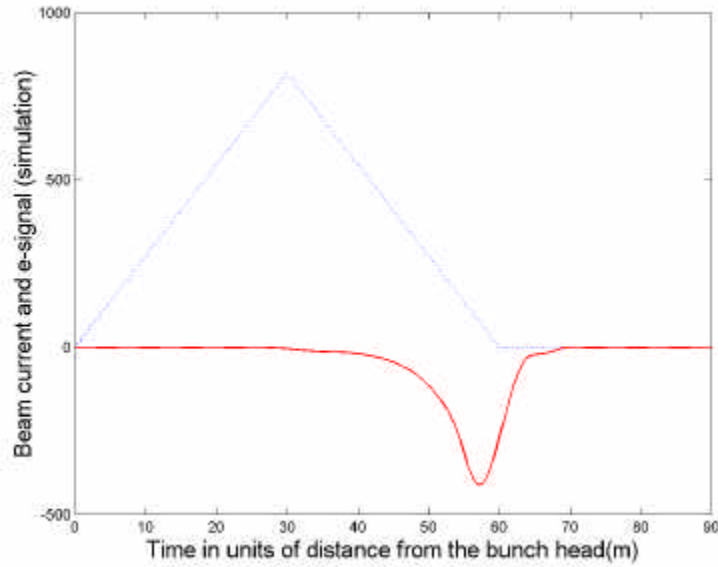


Figure 3 Proton bunch longitudinal distribution (blue) and the electron signal (red).

Fig. 3 shows the simulated electron signal (red line) in arbitrary units (since we don't have electron space charge or any other mechanism, opposing to electron accumulation). The initial electrons are distributed uniformly along the ring at the vacuum chamber wall and the proton bunch density is a triangular with the total length of $2/3$ of the ring (90 meters). The total number of particles is taken to be $3 \cdot 10^{13}$ and the maximum secondary emission coefficient is 2, which roughly corresponds to the stainless steel vacuum chamber. The form of the electron signal is more or less evident. Electron density builds up on the trailing edge up to the point where the proton density is not big enough to give the electrons energy sufficient enough to produce the avalanche. From this point near the end of the proton bunch, the electron density goes down. Figure 4 shows the SEM factor (multiplication of electron density from the center to the end of the proton bunch) for various materials. For large maximum SEM coefficients (y_{\max} in (1)) the SEM factor is roughly proportional to $(y_{\max})^{1/3}$.

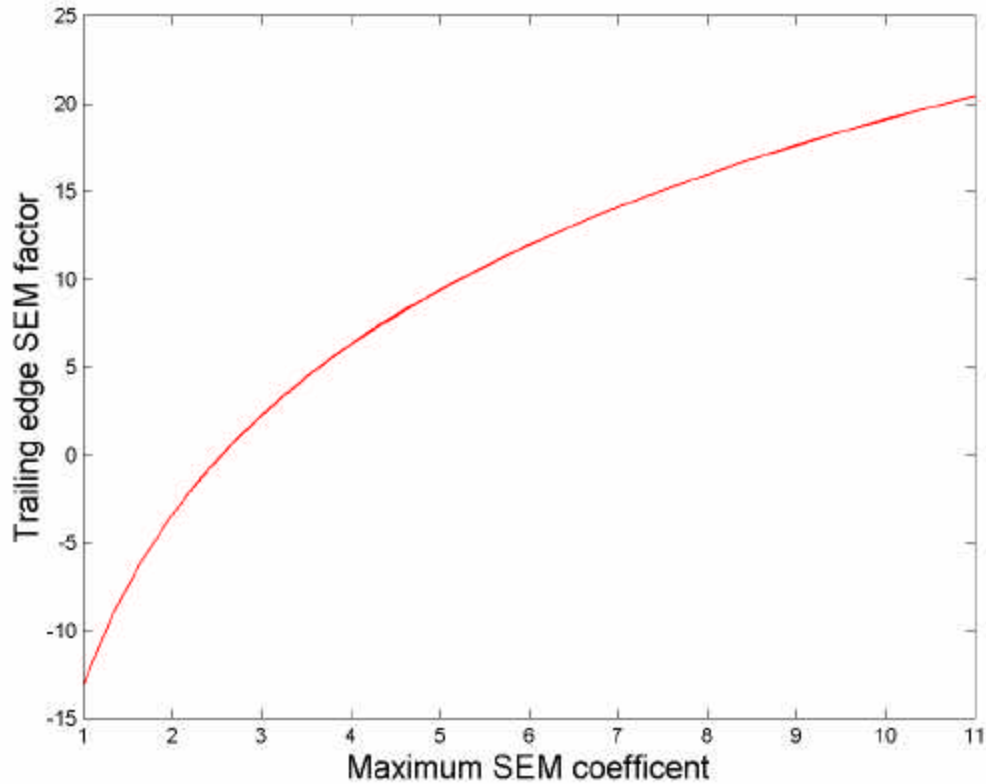


Figure 4 The secondary emission factor versus the maximum SEM coefficient of various materials.

The instability adds its own signatures to the electron signals. Figure 5 shows electron signals for the proton beam's unstable motion with the instability starting at about 3000th turn. The initial electron signal (blue line with the negative polarity) is near the end of the proton bunch (WCM signals stand for longitudinal proton beam current). Then the signal moves toward the center of the proton beam. Our hypothesis is that this behavior is related to the oscillations of the beam centroid. As instability develops, the unstable oscillations move toward the center of the beam. These oscillations drive the electrons to the vacuum chamber wall and we see the same forward movement of the electron signal along with the same movement of the centroid oscillations of the proton beam. The reason for the shift of the unstable part of the proton beam toward the center is not perfectly clear.

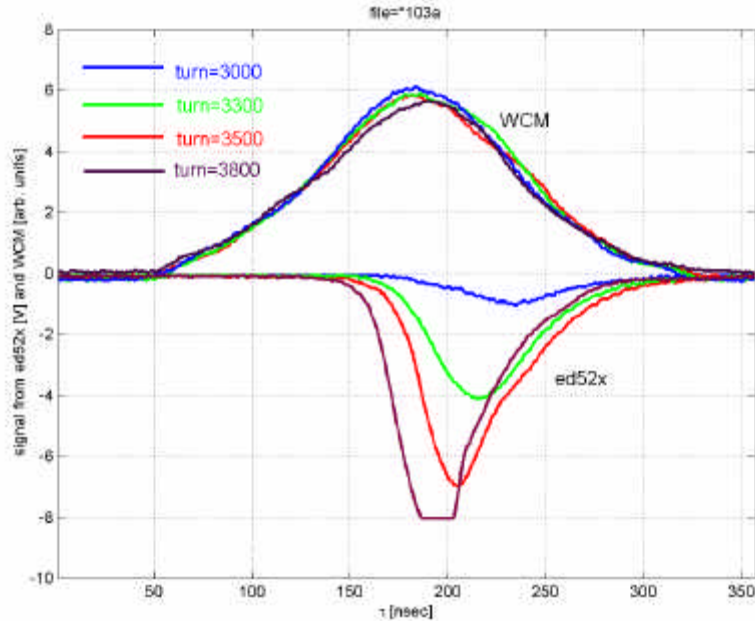


Figure 5 Electron signals at several stages of instability development

MULTI-TURN ELECTRON ACCUMULATION

The multi-turn electron accumulation is a more complicated phenomena than the single pass accumulation. It significantly depends not only on the SEM coefficient but also on the energy and angle distribution of the secondary electrons, the proton beam gap length, the amount of beam in the gap, etc. To explain the main idea it is worth first to use a simple model. Let's imagine that the proton beam has a rectangular longitudinal distribution and a uniform transverse distribution (see Figure 6).

The electron energies outside the proton beam are determined by the energy distribution of the secondary emission electrons. Since these energies are small when compared to the electric potential of the proton beam, inside the proton beam the electrons start to oscillate by cosine law and have the maximum kinetic energy up to several keV, depending on the beam intensity. For example, the electric potential at the center of the PSR proton beam is about 5 kV. At the end of the proton beam the frequency and the bunch length determine electron transverse oscillation phase. If we took a 90 degree electron phase advance, the electron energy at the end would correspond to 5 keV. Figure 6 approximately corresponds to the case described above. High-energy electrons hit the vacuum chamber immediately after the proton bunch, producing the secondary particle avalanche. The secondary particles have much

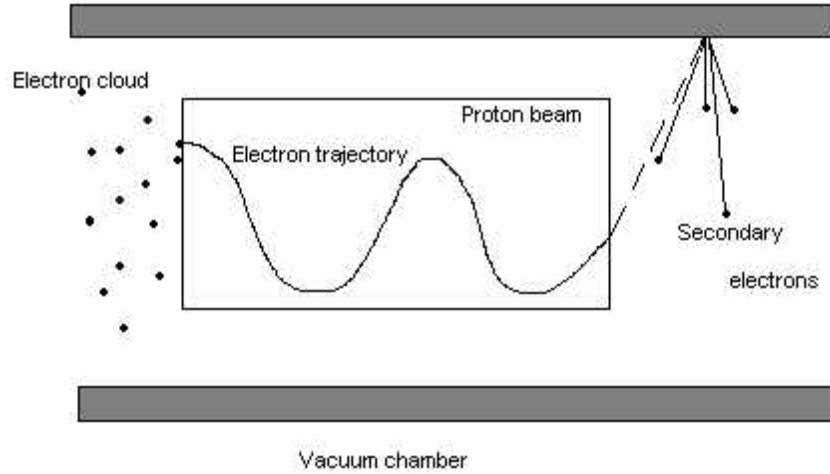


Figure 6 Schematic motion of electrons in the field of the proton bunch.

lower energies than the primary electrons, so they drift slowly in the gap, forming the nonuniform cloud. The most energetic of them hit the wall in the gap with low probability to produce the secondary electrons. Others particles survive the beam gap and repeat the described process again. When the electron cloud density is big enough to repulse the secondary particles back into the wall, the accumulation saturates.

To study more complicated nonlinear electron dynamics, the code for the single pass multipacting (see previous section) was modified. The electron dynamics in the fields of the proton beam was left the same. The proton beam was assumed to have the Gaussian transverse distribution with its r.m.s. equal to 2 cm. For the secondary emission coefficient we use a more detailed formula than Formula 2:

$$y(E) = y_{\max} 1.11(E/E_m)^{-0.35} (1 - e^{-2.3(E/E_m)^{1.35}}) / \cos \mathbf{q} \quad (3)$$

It includes $\cos \mathbf{q}$ in denominator, where \mathbf{q} is the angle of incoming particle with the surface normal vector. This angle was assumed to be zero for the multipacting on the trailing edge for simplicity, but the multi-turn accumulation mechanisms are more delicate, and we should include some longitudinal electron velocities in order to get more realistic picture. Since we have only one-dimensional simulation, we should make some assumptions on the electron longitudinal velocities to calculate the angle \mathbf{q} in (3). Because of the longitudinal fields of the proton beam and even small dispersed magnetic fields in straight section of the real accelerator, the transverse velocity in the beam gap could be transferred to the longitudinal direction. It is reasonable to assume that the longitudinal velocities are of the same magnitude as the transverse ones. Once the electron hits the vacuum chamber, its transverse velocity is taken from the simulation of its motion in the fields of the proton beam. Its longitudinal energy is taken randomly in the range from zero up to the energy of 40 eV (this number is close to the average transverse energy of the electrons while they hit the wall). The distribution of the secondary electrons is another not very certain parameter. This

distribution can vary hundreds of percents depending on the surface conditioning, its cleanliness, its material, etc. Some measured distributions for metals have the form $f(E)=1/(\sigma^2 + (E-E_0)^2)$, with σ of about 3.5 eV and $E_0 \approx 1.5$ eV¹¹. We use this energy distribution for our simulations.

Electrons with such small energies can survive the gap. For example, if the electron had the energy of 2 eV and its velocity is perpendicular to the vacuum chamber, it would barely cross the 5 cm radius vacuum chamber during the beam gap (correspondent time is $30\text{m}/\beta c = 119$ ns). Thus, the most energetic electrons can still hit the wall during the proton beam gap duration. They will not disappear completely, however they produce secondary emission electrons again, but much smaller number because of their small energies. For example, for aluminum the number of secondary emission electrons, produced by one incoming electron is about 0.05, and there is probability of about 0.2 for electrons to bounce back from the wall. Finally, the low energy electron cloud in the gap consists of low energetic electrons as a result of single or multiple electron collisions with the vacuum chamber. For a high space charge electron cloud part of the electrons repulsed back to the wall and low energetic electrons can not hit the wall a second time. The electron detector for this case should measure only primary electrons signal.

The maximum SEM is taken to be $y_{\max} = 2.5$ (this roughly corresponds to the unconditioned stainless steel surface) for the next figures. The set of other parameters we use for the tracking is shown in Table 1:

Proton kinetic energy, E_k	0.8 GeV
Circumference, C	90 m
Longitudinal triangular distribution length, L	60 m
Number of protons, N	$4 \cdot 10^{13}$
Vacuum chamber radius, R	0.05 m
Beam radius, r_b	0.02 m

Table 1 PSR parameters for simulations

We track one particle for 1000 turns and add up all the signals for averaging. Figure 7 shows the electron signal in the electron detector for the small electron density (small means the voltage in the center of the electron cloud is less than 1 V). One can see that there is very good agreement of the signal forms of the experimental data with the data from simulations. The difference of the simulation and the experiment is that the first one gives several times higher accumulation rates of the electron cloud. For the simulations this time is about 10-100 turns, while the experiments give typically 300 turns for accumulation time. Probably, more realistic 3D simulation could reproduce the accumulation time with a greater accuracy.

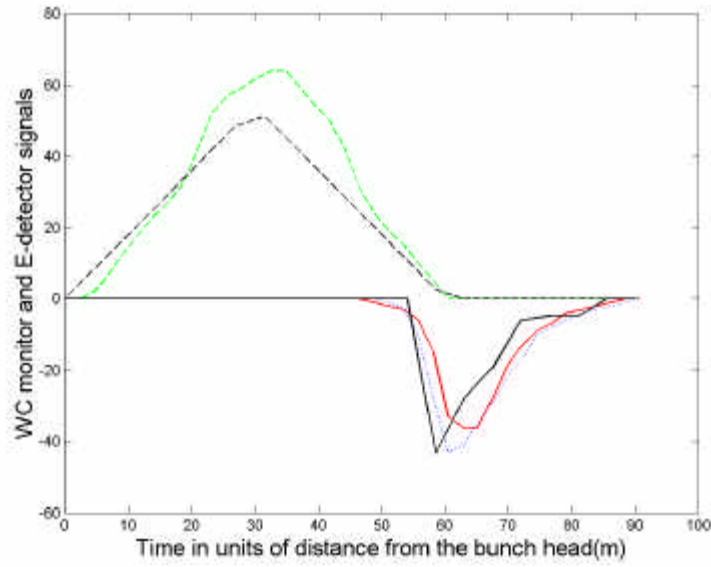


Figure 7 Experimental signals (green line is a Wall Current monitor signal, blue corresponds to the horizontal, and red - to the vertical electron detector) and simulated signal (black solid line) for the same intensity for triangular distribution (black dashed line).

This accumulation mechanism depends strongly on the proton beam distribution. If the distribution is triangular, the electron energy at the end of the bunch would be much less than in the rectangular distribution case. We investigated various distributions with different

smoothness. As a trail distribution function, the expression $C \cdot \left(1 - \frac{s^2}{L_b^2}\right)^m$ is chosen. The

constant parameter C is adjusted to keep the number of particles independent of μ . The larger μ , the smoother the distribution function. Figure 8 presents electron signals (solid lines) and distributions for the set of $\mu=1$ (red), 2(blue) and 5(green). One can see that for more smooth distributions (with larger μ) the electron signals gets smaller with its width larger. As for the limiting case, the electron motion is stable for the long gaussian proton bunch and the accumulation by means of multipacting is absent completely (one can find the discussion of this problem in¹²). This strong dependence on the proton bunch distribution is a typical feature of the e-p instability.

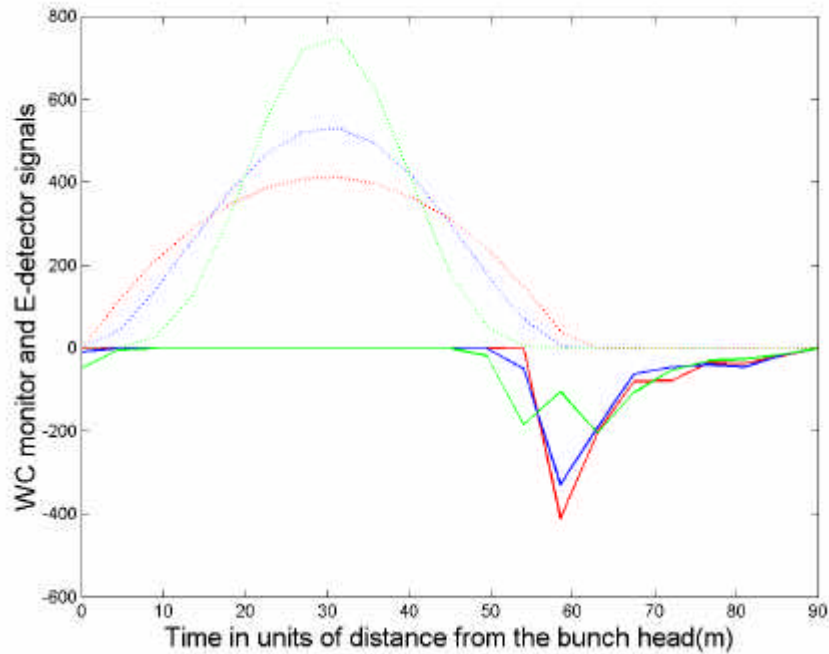


Figure 8 Simulated electron signals (solid lines) for various proton beam distributions (dashed lines) with the same number of particles ($3 \cdot 10^{13}$ protons).

LEVELS OF SATURATION

The single pass accumulation mechanism can produce the immense amount of electrons and the electron cloud density could be comparable with that of the proton beam. That is why the insertions with ceramic or aluminum are very undesirable for accelerators of this type. As for the multi-turn accumulation, the saturation level is much lower. Let's do the simple estimation: let's assume that the electron density is close to saturation when the low-energy electrons have time to return back to the wall during the proton beam gap due to the own space charge fields. Let's denote the ratio of average linear densities of the electron cloud and the proton beam as c (one can call it the degree of electron compensation). We assume the beam gap is $1/3$ of the ring circumference. We can make a simple estimation for the constant electric field of the electron cloud near the wall. After equating gap duration to the time needed for an electron to get back to the chamber, one can get the degree of compensation $c = 0.003\sqrt{E_{out} (eV)}$, where E_{out} is the energy of the secondary electron. If we take it as equal to r.m.s. energy of 3.5 eV, it will give us $c=0.56 \cdot 10^{-2}$ or less than one percent. But still, that could be enough for instability to occur. Below we present more detailed calculations on steady state conditions of the electron beam in the gap and the influence of the proton beam in the gap on electron accumulation levels.

Now we consider self-consistent motion of the electron cloud in the gap. Just after the bunch passes there is a cloud of electrons, which will expand without the confining force of the proton electric field. For an order of magnitude estimate take a uniform, cylindrical, initial density, n_0 with negligible velocity. The electron electric field increases linearly with radius inside the cloud and the cloud will expand in a self-similar way. Let the cloud radius be r , then

$$m_e \frac{d^2 r}{dt^2} = \frac{e \lambda_e}{2 \pi \epsilon_0 r}, \quad (4)$$

where λ_e is the (constant) electric charge per unit length. Define $T(r_0)$ to be the time when e^- starting at r_0 reach $r=b$, the wall.

$$T(r_0) = b G(b/r_0) \sqrt{\frac{2 \epsilon_0 m_e}{e^2 n_0 r_0^2}}, \quad G(x) = \frac{1}{x} \int_1^x \frac{dy}{\sqrt{\ln y}}. \quad (5)$$

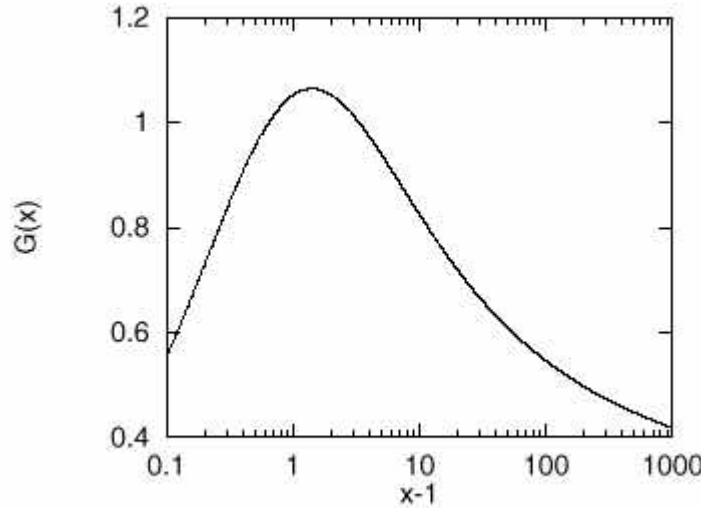


Figure 9 Function $G(x)$ versus $x-1$.

The electron charge per meter at time T after the bunch passage is

$$\Lambda_e = e \pi n_0 r_0^2 = \left(\frac{bG}{cT} \right)^2 \frac{2 \pi \epsilon_0 m_e}{e} = 28 \text{ mC} / m \left(\frac{bG}{cT} \right)^2. \quad (6)$$

The electron density after a gap of duration T depends on the initial density only through G and, as seen from the figure, the value of G is between 0.4 and 1 for a broad parameter range. Taking PSR parameters of $T=100 \text{ ns}$ and $b=5 \text{ cm}$, $\Lambda_e = 78 \text{ G}^2 \text{ pC/m}$.

With a 90 m circumference and 3mC of protons the fractional neutralization is 0.23 % for $G=1$.

Now consider the effect of beam in the gap on the PSR instability threshold¹³. About 3 % beam in gap is required to double the threshold buncher voltage for a given proton intensity and bunch length. This suggests that around 1.5 % neutralization is present without beam in the gap and the estimate above is off by a factor of 10, if only single turn accumulation responsible for the electron density. If we assume there is no beam in the gap for normal operations then some other confining potential is required to keep electrons from hitting the wall during the gap. One possibility is that positive ions generated during the passage of the proton bunch will lead to a neutral plasma during the gap. The plasma would contain as many electrons as ions which could lead to a large number of electrons surviving the gap.

To estimate the number of ions consider a debunched beam with current I_b . Let the beam be of uniform density and round with radius a . The rate at which ions are generated per unit volume within the beam is $\dot{n}_i = \mathbf{s} n_p n_g v_b$, where $n_p v_b = I_b / (\mathbf{p} a^2 e)$ is the proton flux. To get the steady state ion distribution within the beam, assume that the electric fields from the ions and electrons are negligible. This leads to a radial electric field $E = Z_0 I_b r / (2\mathbf{p} a^2)$. The equation of motion for a single ion within the beam is then

$$\frac{d^2 r}{dt^2} = \frac{q_i E}{m_i} \equiv \frac{r}{\mathbf{t}_i^2}, \quad (7)$$

Where q_i is the ion charge and m_i is the ion mass. For an ion created at radius r_0 at time $t=0$ its radial position evolves according to $r = r_0 \cosh(t/\mathbf{t}_i)$, as long as $r < a$. Consider the set of ions generated in the interval $(\mathbf{t}, \mathbf{t}+d\mathbf{t})$. They will have an initial number density of $dn = \dot{n}_i d\mathbf{t}$ and as time progresses this number density will decrease because of expansion in the radial electric field. Since the field varies linearly with radius the expansion is self-similar within the beam. If we limit our attention to the region within the beam then

$$dn(t) = \frac{dn(\mathbf{t})}{\cosh^2\left(\frac{t-\mathbf{t}}{\mathbf{t}_i}\right)}$$

Adding up the contributions to the density for all $\mathbf{t} < t$ gives

$$n_{in} = \dot{n}_i \int_{-\infty}^t \frac{d\mathbf{t}}{\cosh^2\left(\frac{t-\mathbf{t}}{\mathbf{t}_i}\right)} = \dot{n}_i \mathbf{t}_i.$$

The situation outside the beam is more complicated but an upper limit can be made by noticing that the electric field due to the beam always leads to $\ddot{r} > 0$. Hence, an upper limit to the density is obtained by assuming a constant radial velocity outside the beam

giving $n_{out} \ll n_{in}a/r$. Integrating over the pipe cross section of radius b leads to the total number of ions in the ring,

$$N_p n_g s v_b t_l \leq N_{ion} \leq N_p n_g s v_b t_l (2 \frac{b}{a} - 1).$$

The coefficient $n_g s v_b = I/t_p$ has been estimated previously, $t_p \geq 100$ ms. To estimate t_l take $I_b = 20$ A, $a = 2$ cm, $q_i = e$ and $m_i = 28 m_p$, appropriate to singly ionized carbon monoxide. Then $t_l = 312$ ns. For $b/a = 3$, $N_{ion}/N_p \leq 1.6 \times 10^{-5}$. This is two orders of magnitude smaller than the neutralization predicted by the free expansion of the electrons.

Along with the protons in the beam there are the electrons generated on the tail of the bunch. While the dynamics is complicated the net ionization produced by the electrons can be estimated knowing the number of electrons detected at the wall per unit area per turn. Let $Q = Q_9$ nC/cm² be the charge collected per square centimeter per turn at the pipe radius. Assuming a radial flow the time average electron flux is

$$n_e v_e = \frac{Qb}{e T_{rev} r} = Q_9 \frac{b}{r} 1.75 \times 10^{20} m^{-2} s^{-1}.$$

For comparison purposes a 20 A proton beam yields an average flux within the pipe of $1.59 \times 10^{22} m^{-2} s^{-1}$. Typical data¹⁴ give $Q_9 \leq 1$ so it is unlikely that ions generated by either the proton beam or the multipacting electrons are able to confine a significant electron density through the gap.

To gain confidence in the order of magnitude estimates made in this section some numerical simulations were performed. They included electron multipacting and space charge of both the proton and electron beams. The simulation had cylindrical symmetry with no magnetic fields. The electron line density as a function of time for various values of the beam charge density in the gap are plotted in Figure 10. The constant line $G=1$ corresponds to equation (6) evaluated for $G=1$. Other parameters include an average beam current of 20 A, a beam radius of 2 cm, a pipe radius of 5 cm, and a gap length of 100 ns. The current profile was taken to be a semi-circle.

The above calculations suggest that multiturn mechanism alone can't explain instability and "beam in the gap" phenomena. We assume that single pass mechanism give a big contribution in the total electron density. To explain the threshold dependence of the threshold on the proton beam in the gap, the single pass e-accumulation (which doesn't depend on proton beam in the gap) should produce more than 50% of the total electron density. In this case the multiturn e-accumulation is less influential and this fact can quantitatively explain "beam in the gap" phenomena.

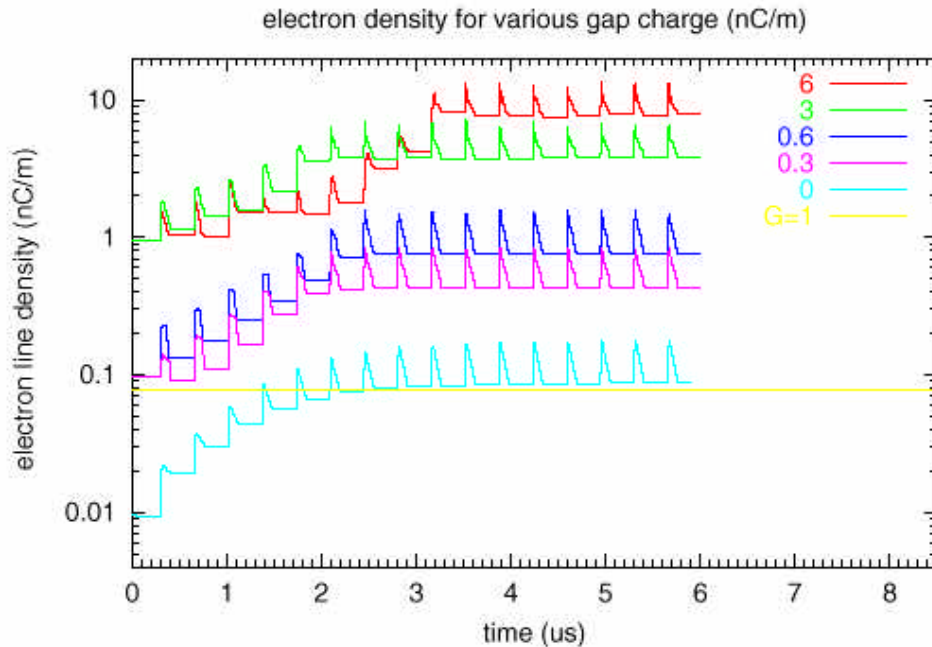


Figure 10 Electron line density versus time for various amount of proton beam in the gap.

CONCLUSION

It is shown that the multipacting process could be a major factor in the electron accumulation in the PSR. Two mechanisms of the multipacting are described. In some aspects of the process, the agreement of theoretical predictions and the experiments turns out to be satisfactory.

ACKNOWLEDGEMENTS

The authors acknowledge the support of the Division of Material Science, U.S. DOE, under contract number DE-AC05-96OR22464 with LMER Corp. for ORNL, and are grateful to Robert Macek for offering the experimental data and for the organization of the PSR experiments on e-p instability. Special thanks go also to Berkley and SLAC physicists, namely, Richard Gough, Roderick Keller, Kurt Kennedy, Lowell Klaisner, and Roland Yourd for conducting of Ti N coating for the PSR vacuum chamber pieces. The authors thank Justin Jones and Sushil Sharma for their preparation of the vacuum chamber spool pieces, and Andrew Browman for providing explanations on details of the experiments with the electron detectors. We are grateful to Robert Kustom and David Olsen for their help and the support of all these activities and to Mike Plum, Tai-Sen Wang, and Paul Channell for valuable discussions and sharing their ideas on e-p instability.

-
- [¹] M. Blaskiewicz, "Instabilities in the SNS", PAC99, New York, March, 1999
- [²] D. Neufer, et al., NIM A**321**, 1-12 (1992).
- [³] K. C. Harkay and R. A. Rosenberg, "Measurements of the Electron Cloud in the APS Storage Ring", PAC99, New York, 1999
- [⁴] R. Kustom, talk at PSR buncher Workshop, Los Alamos, February, 1999
- [⁵] R. Macek, Santa Fe Workshop 2000.
- [⁶] M. Plum, Santa Fe Workshop 1997.
- [⁷] H. G. Hereward, CERN 71-15 (1971).
- [⁸] M. Blaskiewicz AIP Conf 496, p321.
- [⁹] M. Blaskiewicz, talk in Los Alamos, February, 1999
- [¹⁰] F. Zimmerman, "Electron-Cloud Instability and beam-Induced Multipacting in the LHC and in the VLHC", SLAC-PUB-7664, October 1997
- [¹¹] M. Blaskiewicz, private communication.
- [¹²] S. Heifets, et al., "Comment to the Kinematics of e-p Multipactoring", Workshop on Instabilities of High Intensity Hadron Beams in Rings, Upton, New York (1999)
- [¹³] R. Macek AIP Conf 448, p116.
- [¹⁴] A. Browman, Santa Fe Workshop 2000.